Collinear type II second-harmonic-generation frequency-resolved optical gating for use with high-numerical-aperture objectives

David N. Fittinghoff

Institute for Nonlinear Science, University of California, San Diego, La Jolla, California 92093-0339

Jeff A. Squier

Department of Electrical Engineering and Computer Science, University of California, San Diego, La Jolla, California 92093-0339

C. P. J. Barty

Institute for Nonlinear Science, University of California, San Diego, La Jolla, California 92093-0339

John N. Sweetser and Rick Trebino

Combustion Research, Sandia National Laboratories, Livermore, California 94551

Michiel Müller

BioCetrum Amsterdam, Institute for Molecular Cell Biology, Kruislaan 316, 1098 SM Amsterdam, The Netherlands

Received March 19, 1998

Ultrashort-pulse lasers are now commonly used for multiphoton microscopy, and optimizing the performance of such systems requires careful characterization of the pulses at the tight focus of the microscope objective. We solve this problem by use of a collinear geometry in frequency-resolved optical gating that uses type II second-harmonic generation and that allows the full N.A. of the microscope objective to be used. We then demonstrate the technique by measuring the intensity and the phase of a 22-fs pulse focused by a 20×, 0.4-N.A. air objective. © 1998 Optical Society of America

OCIS codes: 140.7090, 320.7100, 320.7160.

In multiphoton microscopy, determining the optimum exposure conditions, i.e., those that provide the best combination of image resolution, contrast, and specimen viability, requires an accurate picture of the field at focus.[1] Thus a method for accurately determining the pulse intensity and phase at the focus produced by a microscope objective is vital.

Currently, frequency-resolved optical gating[2] (FROG) provides the most sophisticated and reliable pulse intensity and phase measurements. FROG is a suite of techniques that use phase-retrieval algorithms to obtain the intensity and the phase of ultrashort pulses from frequency-resolved autocorrelations of the pulses. The specific FROG geometry required for a measurement depends on the power, wavelength, and other characteristics of the pulse. To date, all FROG devices have relied on noncollinear geometries. For pulses focused by a high-N.A. objective, however, a collinear geometry allows the full N.A. of the objective to be used, producing the tightest focus and, subsequently, the greatest intensity and the highest spatial resolution. Thus, for multiphoton microscopy, it is desirable to use a collinear FROG geometry for measurements at the focus of high-N.A. objectives.

In this Letter we present what we believe to be the first demonstration of a collinear FROG technique, specifically, one based on collinear type II second-harmonic generation (SHG). We describe this variation on the FROG technique and present a measurement of a 22-fs pulse focused by a 20×, 0.4-N.A. air objective by use of type II SHG FROG.

FROG relies on frequency resolving an autocorrelation of the pulse to obtain the signal:

$$I_{\mathrm{FROG}}(\omega, \tau) = \left| \int_{-\infty}^{\infty} E_{\mathrm{sig}}(t) \exp(-i\omega\tau) \mathrm{d}t \right|^2 . \qquad (1)$$

Here $E_{\mathrm{sig}}(t, \tau)$ is the signal field produced by the autocorrelation as a function of time t and time delay τ, and ω is the angular frequency. For noncollinear SHG FROG, the signal field for a plane wave with perfect phase matching is

$$E_{\mathrm{sig}}(t, \tau) = E(t)E(t - \tau) , \qquad (2)$$

where $E(t)$ is the electric field of the pulse that is being measured.

The experimental setup for type II SHG FROG is similar to that for SHG FROG, except that, as shown in Fig. 1, the beams are collinear, and there is a 90° polarization rotation between the two arms of the FROG interferometer. Type II SHG FROG also uses type II phase matching instead of type I phase matching.

0146-9592/98/131046-03$15.00/0

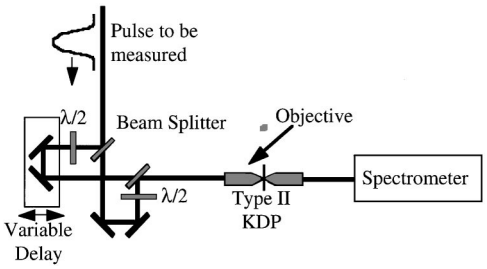

Fig. 1. Schematic of a collinear type II SHG FROG device that is similar to an interferometric SHG FROG, except that there is a 90° polarization rotation between the two arms (achieved by placement of a $\lambda/2$ wave plate in each arm) and that the device uses a type II crystal. In this study the crystal was potassium dihydrogen phosphate (KDP).

Type II SHG FROG has several advantages. Since the signal field for type II SHG FROG is identical to that for SHG FROG, type II SHG FROG traces are identical to SHG FROG traces, and the existing SHG FROG algorithms can be used to retrieve the intensity and phase. One can also produce type II SHG FROG devices from an existing interferometric SHG autocorrelator simply by placing identical zero-order wave plates in each arm of the autocorrelator and replacing the type I crystal with a type II crystal. Also, a minor rotation of the type II crystal produces temporal fringes with a known spacing, making type II SHG FROG self-calibrating in delay. These temporal fringes are those normally associated with interferometric autocorrelation.

Using a collinear geometry has another advantage as well. Current laser systems routinely produce pulses shorter than 30 fs, and several research groups have produced pulse widths of 10 fs or less.[3–5] These pulses are only a few optical cycles long, but careful control of dispersion, group delay as a function of radius in the objective, and other system parameters could potentially allow few-cycle pulses to be focused by microscope objectives. For all noncollinear geometries, the finite crossing angle of the beams produces temporal blurring. For asymmetric FROG geometries, the finite thickness of the nonlinear medium also produces geometrical distortions that produce temporal blurring.[6] Using a collinear geometry eliminates these problems.

There is one important consideration in type II SHG FROG that partially neutralizes this last advantage. In a type II crystal the two different polarizations propagate along different optical axes, and the different propagation velocities along those axes produce a temporal walk-off in the type II crystal between the two polarizations.[7] For a 50-μm-thick type II KDP crystal, the temporal walk-off is approximately 8 fs. Such a large walk-off would badly distort the FROG signal for pulses of $<$50 fs. If the confocal parameter is much shorter than the crystal thickness, however, the effective interaction may be much shorter, which greatly reduces the temporal walk-off. The blurring that is due to the walk-off will usually be negligible for multiphoton microscopy when high-N.A. objectives are used. We note that the short interaction region also increases the effective phase-matching bandwidth. Alternatively, shorter crystals could be used.

An unusual feature of the method presented in this Letter is the use of a nonlinear medium that is thick compared with the light Rayleigh range. All previous FROG measurements have used thin media. However, all pulse-measurement techniques require that the pulse field be separated into the product of time- and space-dependent functions. As a result, the (spatial) thick-medium effects factor out of the temporal integral for the FROG trace and reside in a spatial integral, which is constant with respect to delay and plays no role in the trace.

To demonstrate type II SHG FROG, we measured 22-fs pulses from a Ti:sapphire oscillator. For the measurement, we used a 20$\times$ air objective with a N.A. of 0.4 and a 50-μm-thick type II KDP crystal. We set the focus just inside the surface of the crystal by monitoring the intensity and scanning the position of the crystal. The confocal parameter in this case is $\sim$10 μm, leading to a temporal walk-off in the crystal of 1.6 fs. Since the effect of the walk-off is a convolution of the intensity over this region, the actual distortion should be lower. We rotated the polarization by use of two zero-order $\lambda/2$ wave plates, one in each arm of the dispersion- and amplitude-balanced autocorrelator. As an alternative, we could have rotated the polarization by use of an out-of-plane rotation. In this experiment the FROG trace did have residual fringes that were approximately 10% of the peak for each wavelength, owing to the wave plates. These fringes existed because the polarization of the beams was not extremely pure owing to the lack of polarizers, which would have eliminated residual incorrect polarization. Since the pulse duration in this Letter corresponded to many optical cycles, we used Fourier low-pass filtering along the time axis of the FROG trace to remove the residual fringes. The measured FROG trace is shown in Fig. 2. The pulse was retrieved well, with a FROG error of 0.0032 for a 128 $\times$ 128 pixel trace. Figure 3 shows the retrieved intensity and phase of the pulse as a function of time. The FWHM of the intensity is 22 fs, and the FWHM of the spectrum is 63 nm.

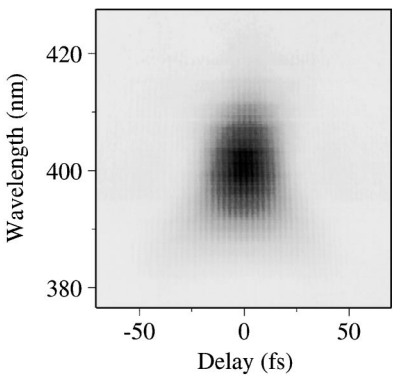

Fig. 2. Measured type II SHG FROG trace of a 22-fs pulse from a Ti:sapphire oscillator taken by a 20$\times$, 0.4-N.A. air objective. The residual fringes shown in these raw data disappear after Fourier filtering.

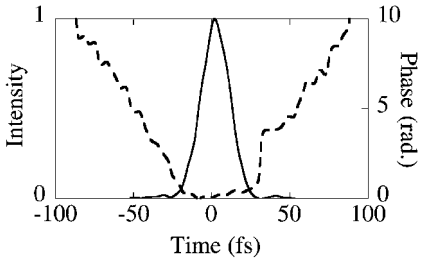

Fig. 3. Retrieved intensity and phase for the type II SHG FROG trace shown in Fig. 2.

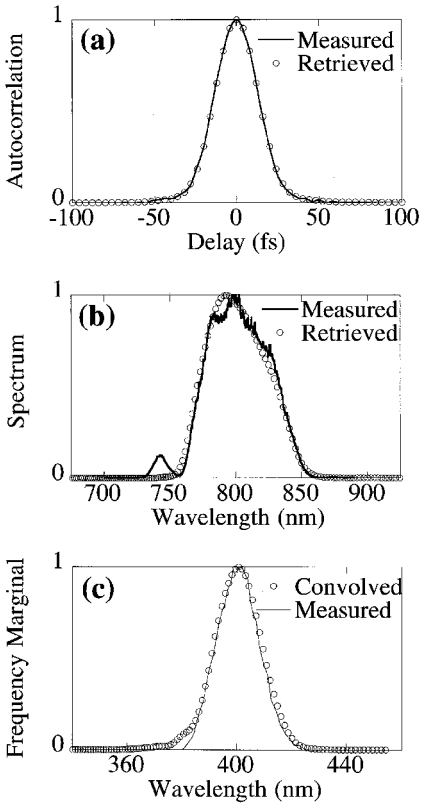

Fig. 4. (a) Measured and retrieved SHG autocorrelations. (b) Measured and retrieved spectra. Note that the small subpeak in the measured spectrum at 740 nm is due to mode-hopping cw lasing in the Ti:sapphire oscillator and should not appear in the retrieved spectrum because the nonlinearity of the FROG device is insensitive to low-power signals. (c) Measured frequency marginal of the FROG trace and the autoconvolution of the measured spectrum (Convolved). Again note that the only significant deviation is the wing of the autoconvolution near 370 nm that is produced by the cw subpeak.

The 0.62-FWHM time–bandwidth product occurs because of the high-order residual phase distortions, which are not corrected for by our precompensating compressor. As shown in Fig. 4, the retrieved SHG autocorrelation and spectrum agreed well with the separately measured autocorrelation and spectrum, and the measured frequency marginal of the FROG trace and the autoconvolution of the pulse spectrum also agreed well.

For completeness, we note that there are other collinear geometries that will also prove useful. Interferometric second-harmonic generation and interferometric third-harmonic-generation FROG are simply collinear versions of the standard second- and third-harmonic-generation FROG techniques,[2] respectively, that build directly on the established strengths of interferometric SHG and interferometric third-harmonic generation autocorrelation. Ultimately, because of the fringe-resolved capability and the freedom from temporal blurring and geometrical distortions of these techniques, they may prove to be the best methods for measuring pulses of only a few optical cycles. These techniques require new algorithms, however, which are under development.

In conclusion, we have demonstrated for what we believe to be the first time a collinear FROG geometry that allows the full N.A. of a microscope objective to be used. This technique will be particularly useful for measuring pulses at the foci of objectives used for ultrafast multiphoton microscopy, where using the full N.A. of the focusing objective produces the tightest focus and, subsequently, the highest spatial resolution. We have used type II SHG FROG to measure 22-fs pulses from a Ti:sapphire oscillator that have been focused by a 20×, 0.4-N.A. air objective.

References

1. M. Müller, J. Squier, R. Wolleschensky, U. Simon, and G. J. Brakenhoff, "Dispersion pre-compensation of 15 femtosecond optical pulses for high-numerical aperature objectives," J. Microsc. (to be published).
2. R. Trebino, K. W. DeLong, D. N. Fittinghoff, J. N. Sweetser, M. A. Krumbugel, B. A. Richman, and D. J. Kane, Rev. Sci. Instrum. **68,** 3277 (1997).
3. G. Taft, A. Rundquist, M. M. Murnane, I. P. Christov, H. C. Kapteyn, K. W. DeLong, D. N. Fittinghoff, M. A. Krumbügel, J. N. Sweetser, and R. Trebino, IEEE J. Select. Topics Quantum Electron. **2,** 575 (1996).
4. I. D. Jung, F. X. Kartner, N. Matuschek, D. H. Sutter, F. Morier-Genoud, G. Zhang, U. Keller, V. Scheuer, M. Tilsch, and T. Tschudi, Opt. Lett. **22,** 1009 (1997).
5. S. Sartania, Z. Cheng, M. Lenzner, G. Tempea, C. Spielmann, F. Krausz, and K. Ferencz, Opt. Lett. **22,** 1562 (1997).
6. A.-C. Tien, S. Kane, J. Squier, B. Kohler, and K. Wilson, J. Opt. Soc. Am. B **13,** 1160 (1996).
7. A. M. Weiner, IEEE J. Quantum Electron. **QE-19,** 1276 (1984).